Rational material design of mixed-valent high T_c superconductors

Z. P. Yin[1] and G. Kotliar[1]

[1] *Department of Physics and Astronomy, Rutgers University, Piscataway, New Jersey 08854, United States.*

PACS 74.70.-b – Superconducting materials other than cuprates
PACS 74.20.Pq – Electronic structure calculations
PACS 74.25.Kc – Phonons

Abstract – We design, from first principles calculations, a novel family of thallium halide-based compounds as candidates for new high temperature superconductors, whose superconductivity is mediated by the recently proposed mechanism of non-local correlation-enhanced strong electron-phonon coupling. Two prototype compounds namely $CsTlF_3$ and $CsTlCl_3$ are studied with various hole doping levels and volumes. The critical superconducting temperature T_c are predicted to be about 30 K and 20 K with ∼0.35/f.u. hole doping and require only modest pressures (∼10 and ∼2 GPa), respectively. Our procedure of designing this class of superconductors is quite general and can be used to search for other "other high temperature superconductors".

Introduction. – The holy grail of theory and computation assisted material design is to accelerate the discovery and synthesis of new materials with specific desirable properties. With the rapid development of theory, algorithms, computer codes, and high-performance computers in the recent years, this goal is within reach for materials and properties which are firmly understood with well established tools. In the past two decades, first-principles calculations have been used to look for better functional materials such as batteries and energy storage materials [1, 2], spintronics [3], alloy catalysts [4], multiferroic and magnetoelectric materials [5,6], etc. The topological insulators and Weyl semimetals, which are under current extensive investigations, were first predicted by theory and first-principles calculations. [7–9]

An even more ambitious goal is to approach computational material design in problems, such as reaching higher temperature superconductivity, where there is yet no consensus on the basic mechanisms operating in various classes of materials. Still, given an understanding of a mechanism, modern electronic structure tools can be put to use, and this process in conjunction with subsequent experiments, serves to test our basic understanding of the phenomena and the state of the art of existing algorithms and codes. Numerous attempts have been made to look for high T_c superconductors in hydrogen-rich materials such as SiH_4 [10], $SiH_4(H_2)_2$ [11], and pure hydrogen [12] under high pressure as well as MgB_2-like materials such as LiBC [13], to name a few.

In a recent paper [14], Yin *et al.* found that the electron-phonon coupling in a broad class of materials is significantly enhanced over the value calculated by density functional theory (DFT) in the local density approximation (LDA). This mechanism explains the presence of superconductivity in materials whose mechanism is not magnetic, but nevertheless the standard implementations of the Migdal-Eliashberg theory using LDA computed parameters fail to account for the high T_cs. These "other high temperature superconductors" [15], such as the bismuthates and the transition metal chloronitrides, superconduct at high temperatures as a result of a non-local correlation-enhanced strong electron-phonon coupling. [14] The approach proposed in ref. [14] passed several stringent tests. It is able to explain both high temperature superconductivity as in $Ba_{1-x}K_xBiO_3$ [16] and low/vanishing temperature superconductivity as in the $Ba_{n+1}Bi_nO_{2n+1}$ family with small n [17]. The variation with ions and doping dependence of T_c in the HfNCl family [18] also has a natural explanation within the approach. [14] This class of materials superconduct in close proximity to a metal-insulator transition-a region which is empirically propitious for high temperature superconductivity. In this region, LDA overestimates the screening yielding an estimate of the coupling to the phonon vibrations much smaller than its actual value. An accurate description of the electronic structures and lattice dynamics of this class of materials requires treatment of correlation effects beyond LDA and is fulfilled by the GW method and

the HSE06 [19] *screened* hybrid functional DFT. To evaluate the realistic electron-phonon coupling, Yin *et al.* [14] proposed a simple but efficient approach that combines the LDA linear response calculations and the GW and/or *screened* hybrid functional frozen phonon calculations.

Motivated by the above study [14], in this letter, we put this approach to the test, by using it to search for potential candidates of high temperature superconductors in the mixed-valent class similar to the bismuthates. We identify a new class of thallium halide compounds which can readily form, and has potential for superconductivity of about 30 K.

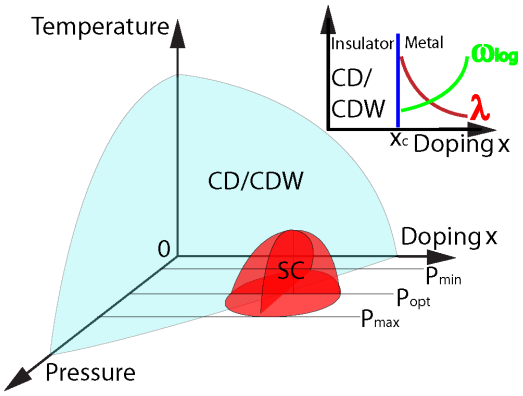

Fig. 1: (Color online) **The schematic phase diagram of mixed-valence compounds such as $BaBiO_3$ and $CsAuCl_3$.** At low pressure and small doping, the compounds have structural distortions and are in the charge disproportionation (CD)/charge density wave (CDW) insulating phase. With enough doping and pressure, the structural distortions and charge disproportionation can be suppressed and they may enter the superconducting (SC) phase. The insert shows the doping dependence of the electron-phonon coupling λ and average phonon frequency ω_{log} in the metallic phase.

General phase diagram. – We search for superconductivity near a charge disproportionation/charge density wave/valence instability. The generic schematic phase diagram is shown in fig.1 and describes (Ba,K)BiO_3. With small doping and at ambient pressure and low pressure, the compounds exhibit structure distortions and are in the charge disproportionation (CD)/charge-density wave (CDW) insulating phase. With sufficient doping and/or at high pressure, the structure distortions and charge disproportionation can be suppressed and the compounds enter the metallic phase and possibly the superconducting phase at low temperature. Moreover, superconductivity may occur only in some range of doping and pressure. Therefore, to achieve the highest superconducting T_c, both the pressure and doping need to be optimized.

General procedure and computational method. – In this work we look specifically for a class of $BaBiO_3$-like compounds satisfying the following criteria: (1) the parent compound is an insulator and contains mixed-valent cations such as Bi (Bi^{3+} and Bi^{5+}), Au (Au^{1+} and Au^{3+}) and Tl (Tl^{1+} and Tl^{3+}); (2) the properly doped compound is metallic and has strongly phonon-coupled bands across the Fermi level. (1) and (2) suggest the compound is a potential "other high-temperature superconductor" like (Ba,K)BiO_3, and can be checked by band structure and linear response calculations where the T_c can be estimated using the approach invoked in ref. [14]. In addition, we try to determine the energetics of the compounds. Ideally, one needs to verify that the proposed compound is energetically favorable among all possible competing phases including elements, binaries, etc. [20]. However, it is impossible to try all the possibilities. In practice, we check the following two conditions: a) the proposed compound should not be very energetically unfavorable relative to the reactants [20] and b) the proposed compound is dynamically stable, i.e., no unstable phonon modes.

With these considerations in mind, we use density functional theory calculations and linear response calculations to design new materials, check their stabilities, and estimate the electron-phonon coupling and the superconducting T_c using the approach proposed in ref. [14].

From starting materials to new materials. – A heuristic reasoning leading to our new materials is the following: $CsTlCl_3$ and $CsTlF_3$ are isostructural with $BaBiO_3$ and share the same valence electron counting as $BaBiO_3$, thus they retain essentially the same band structure around the Fermi level as $BaBiO_3$. With these critical similarities with $BaBiO_3$, superconductivity is expected when $CsTlCl_3$ and $CsTlF_3$ are optimally doped to suppress the structural distortion. Considering the isotope effect, $CsTlF_3$ can have better superconductivity than $CsTlCl_3$.

Alternatively, we can start from the existing $CsAuCl_3$ family [21] and compare it to the celebrated $BaBiO_3$ family. While both families crystallize in the (distorted) perovskite structure and contain mixed-valent cations Bi (Bi^{3+} and Bi^{5+}) and Au (Au^{1+} and Au^{3+}), the parent $BaBiO_3$ compound has oxygen-breathing distortion (arrows in fig.2a) whereas the parent $CsAuCl_3$ displays Cl Jahn-Teller distortion (arrows in fig. 2b). Moreover, unlike the $BaBiO_3$ family with superconducting T_c up to 32 K in optimal doped (Ba,K)BiO_3 [16], no superconductivity has been found in the $CsAuCl_3$ family after extensive experimental searches, even under high pressures. [21, 22]

Since a non-local correlation-enhanced electron-phonon coupling is responsible for the superconductivity in (Ba,K)BiO_3, an evaluation of the electron-phonon matrix elements of $CsAuCl_3$ is helpful to understand the absence of superconductivity in the $CsAuCl_3$ family. Figure 2c shows the band structures of $CsAuCl_3$ in the perfect perovskite structure and with the Cl breathing and Jahn-Teller distortions calculated by VASP [23] with generalized gradient approximation [24] (GGA). With the Cl breathing/Jahn-Teller distortion, the largest band splitting near the Fermi level occurs around L/W point, giv-

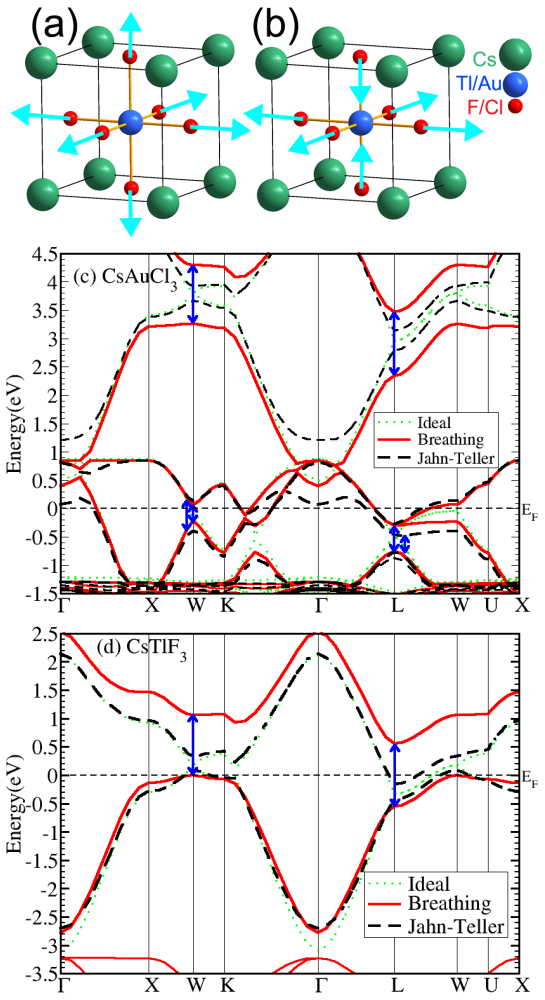

Fig. 2: (Color online) **The crystal structure and band structures of $CsAuCl_3$ and $CsTlF_3$.** (a) and (b) shows the crystal structure of simple cubic perovskite $CsAuCl_3$ and $CsTlF_3$ with arrows showing (a) the F/Cl breathing distortion and (b) the F/Cl Jahn Teller distortion. The corresponding band structures at ideal structure (simple cubic) and with the F/Cl breathing and Jahn-Teller distortions are calculated by DFT-GGA and shown in (c) for $CsAuCl_3$ at a=5.35Å and (d) for $CsTlF_3$ at a=4.6 Å, respectively. The arrows in (c) and (d) indicate the magnitudes of the band splittings under the F/Cl breathing and Jahn-Teller distortions, with atomic displacements of about 0.11 Å for $CsAuCl_3$ and about 0.09 Å for $CsTlF_3$ for both distortions.

ing rise to a reduced electron-phonon matrix element (REPME, defined as the ratio of the band splitting at a high symmetry point to twice the atomic displacement of the corresponding phonon mode, see ref. [14] and fig.2c) of 2.1/2.5 eV/Å. These REPMEs *near the Fermi level* in $CsAuCl_3$ are only one third of the DFT-GGA REPME (7.6 eV/Å) of the oxygen-breathing mode in $BaBiO_3$. [14] Such small REPMEs in $CsAuCl_3$ imply weak electron-phonon coupling thus can hardly host decent superconductivity in the $CsAuCl_3$ family.

However, a good superconductor may still be found in the $CsAuCl_3$-like compounds. Notice that for the Cl-breathing distortion, the band splittings near L and W points at about 3-4 eV above the Fermi level are much larger (5.3 eV/Å), about two and half times the corresponding values near the Fermi level, resulting in REPMEs comparable to those found in $BaBiO_3$. It suggests a strong coupling of this band (centered at 3 eV above Fermi level) to the Cl-breathing phonons which can gives rise to a strong total electron-phonon coupling and mediate good superconductivity. The key is to make this band operate at the phonon energy scale, which requires the Fermi level of $CsAuCl_3$ to move up by ∼3 eV through electron doping (∼2 electrons per formula unit (f.u.)). Here we search for compounds with the same perovskite structure but with higher Fermi level. A good choice is to replace Au with Tl since Tl has two more electrons than Au and is also mixed-valent (Tl^{1+} and Tl^{3+}) in the parent compound $CsTlCl_3$. Thus, starting from $CsAuCl_3$, we find a new compound $CsTlCl_3$, which is mixed-valent and has strong phonon coupled bands near the Fermi level, just like the $BaBiO_3$ compound.

Initial inspection. – To obtain a rough estimation of the lattice constants at ambient pressure, we optimize the structure of $CsTlF_3$ and $CsTlCl_3$ in the perfect perovskite structure (i.e., without any distortion) with LDA, GGA and HSE06 functional. The results are 4.64, 4.82, 4.74 Å for $CsTlF_3$ and 5.40, 5.61, 5.53 Å for $CsTlCl_3$, respectively. It is known that LDA usually underestimates the equilibrium lattice constants while GGA overestimates them. The fact that the HSE06 optimized values of the lattice constants lie between the LDA and GGA values suggests the HSE06 functional provides better description of these compounds, similar to the case of $BaBiO_3$ [25].

We next examine the band structures with respects to the F-breathing distortions. As expected, the REPME of the F breathing mode in $CsTlF_3$ with lattice constant a=4.6 Å is large as shown in fig.2(d), about 5.0 eV/Å in DFT-GGA and 8.8 eV/Å in DFT-HSE06. The corresponding REPMEs of $CsTlF_3$ and $CsTlCl_3$ at other lattice constants are shown in table 1 and 2. These large REPMEs indicate a strong electron-phonon coupling of the F breathing mode which is further enhanced by correlation effects, the same as $BaBiO_3$. Therefore the $CsTlF_3$ family can be another member of the "other high-temperature superconductors". [14]

We further find that there is no information on the $CsTlF_3$ and $CsTlCl_3$ compounds in the ICSD database [26], thus they are candidates for new materials. However, the ICSD database [26] has many literature reporting successful synthesis of the A_2TlMF_6 compounds (A is an alkaline metal and M is a metal element other than Tl) which crystallize in the cubic perovskite structure. This suggests it is possible to synthesize the $CsTlF_3$ and $CsTlCl_3$ compounds and other members in this family.

To check the energetic stability, we consider here a possible reaction to synthesize $CsTlF_3$ as an example:

$2CsF+TlF+TlF_3 \rightarrow 2CsTlF_3+Q$, where all the compounds on the left hand side, i.e., CsF, TlF and TlF_3, are readily available experimentally and Q is the emitted energy during the reaction. Our DFT-GGA calculations suggest the reaction releases about 1.1 eV energy per $CsTlF_3$ unit (106 kJ/mol) and confirm that the above reaction is energetically favored. In constrast, we consider also a currently known compound Cs_3TlF_6 and a possible synthesis reaction: $3CsF+TlF_3 \rightarrow Cs_3TlF_6+Q$. This reaction actually absorbs about 1.7 eV energy per Cs_3TlF_6 unit (164 kJ/mol) according to our DFT-GGA calculations. Therefore, $CsTlF_3$ is more energetically favored than the existing Cs_3TlF_6 compound.

Lattice stability and mapping the phase boundary. – Without doping, the $CsTlF_3$ and $CsTlCl_3$ have strong F/Cl breathing distortions which makes the compounds insulating. To make superconductivity possible, the $CsTlF_3$ and $CsTlCl_3$ have to be properly doped and compressed to suppress the lattice distortions.

To check the lattice dynamics and optimize the doping and pressure, we carried out linear response theory (LRT) calculations using the LMTART code [27] with local density approximation functional [28]. The calculations are done using the simple cubic structure with one f.u. per unit cell at a few hole doping levels and with a few lattice constants (pressure) for both compounds. The virtual crystal approximation is used to simulate the doping effect.

In the LRT-LDA calculations, we find for $CsTlF_3$ unstable phonon modes near the zone boundary at lattice constant a=4.6 $\AA$ for all the hole doping levels studied (0.3, 0.35, and 0.4 hole/f.u.), which indicates that the compound is still in the CDW phase with large hole doping. Whereas at a=4.5 $\AA$, there is no unstable phonon mode in $CsTlF_3$ for the corresponding doping levels. LDA and the virtual crystal approximation underestimate the tendency towards charge disproportionation and structural distortion, thus provide a lower bound for the doping at which the material metallizes. This methodology also suggests that applying pressure is an efficient way to suppress them to enter the metallic phase. Using supercell frozen phonon calculations, we further check the dynamic stability of a hypothetical $CsXeTl_2F_6$ compound (a 0.5 hole/f.u. doped $CsTlF_3$) with respect to F breathing distortion. A 2×2×2 supercell is constructed with half of Cs atoms replaced by Xe atoms in order to calculate the phonon frequency of the F breathing mode at R point. The resulting phonon frequency is 23.5 meV in DFT-GGA and 15.2 meV in DFT-HSE06 with lattice constant a=4.5 $\AA$. Therefore, the F breathing distortion/instability in the parent compound at this volume disappears after certain amount of hole doping in both the GGA and HSE06 treatments. The above calculations suggests that the critical lattice constant to induce metallicity and possibly superconductivity lies between 4.5-4.6 $\AA$ for $CsTlF_3$. Similarly, we find the critical lattice constant for $CsTlCl_3$ is about 5.4 $\AA$.

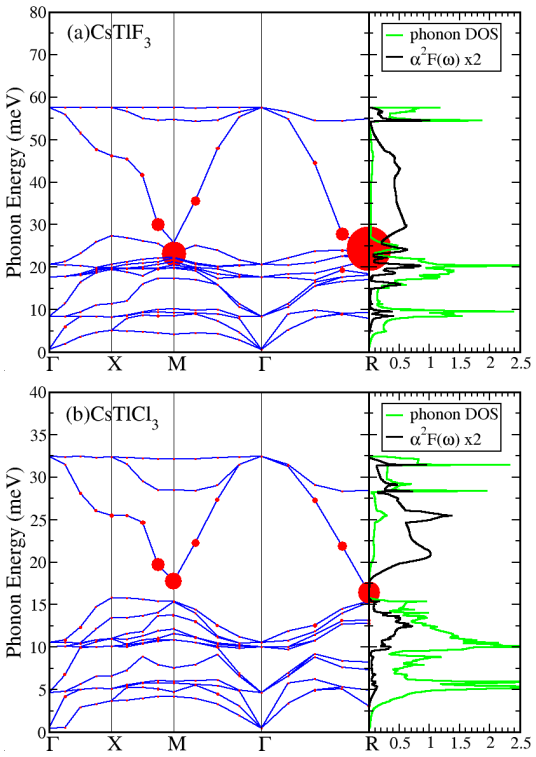

Fig. 3: (Color online) **Lattice dynamics and electron-phonon coupling.** The LRT-LDA calculated (left panel) phonon spectra, mode and momentum-dependent electron-phonon coupling λ whose value is proportional to the radius of the corresponding red dot, (right panel) phonon density of state and $\alpha^2F(\omega)$ of (a) simple cubic $CsTlF_3$ at a=4.5 $\AA$ and (b)simple cubic $CsTlCl_3$ at a=5.3 $\AA$ both with 0.35 hole doping/f.u. (virtual crystal approximation).

Lattice dynamics, electron-phonon coupling, and T_c. – Now we proceed to report the lattice dynamical properties from the LRT-LDA calculations and estimate the electron-phonon coupling λ and the superconducting T_c of hole doped $CsTlF_3$ and $CsTlCl_3$. The LRT-LDA method has been shown to be very reliable in predicting T_c for conventional superconductors [29–32] and is a good starting point for exotic superconductors with correlation-enhanced superconductivity. The LRT-LDA slightly overestimates the average phonon frequency in the "other high temperature superconductors" and we renormalize it by $\sqrt{(1+\lambda)}$. [14] The realistic electron-phonon coupling λ is evaluated from the LRT-LDA calculations and frozen phonon supercell calculations as described in details in ref. [14].

In fig.3, we show the LRT-LDA calculated phonon spectra, phonon density of states and the Eliashberg function $\alpha^2F(\omega)$ for $CsTlF_3$ ($a = 4.50\AA$) and $CsTlCl_3$ ($a = 5.30\AA$) with 0.35 hole doping/f.u.. In the phonon spectra, we denote each frequency at each q point by a dot whose radius is proportional to the mode- and momentum dependent electron-phonon coupling $\lambda(q,\omega)$ of the corresponding phonon mode. All the calculated phonon modes at

Table 1: **The calculated results of selected quantities for simple cubic ATlF$_3$ (A=Cs, Rb, and K).** The displayed items from left to right are the lattice constant a (Å), the corresponding pressure (GPa) for A=Cs, Rb, and K calculated by HSE06 using the simple cubic structure containing 1 f.u., the reduced electron-phonon matrix element (REPME, eV/Å) of the F-breathing mode (see fig.2a and c) calculated by GGA and HSE06, the hole doping level x per formula unit in the LRT-LDA calculations where the virtual crystal approximation is used for doping, the LRT-LDA calculated average phonon frequencies ω_{log} (K), the LRT-LDA calculated electron-phonon coupling λ contributed by optical phonon modes and the total electron-phonon coupling λ, the adjusted total λ for the HSE06 approach, the estimated T_c (K) for LRT-LDA and HSE06 approaches. The lattice dynamical results are based on the assumption that the real material is stable at the proposed doping/pressure/structure. The critical temperatures are obtained from the revised Allen-Dynes formula [33] using μ^*=0.10. The total λ and T_c of HSE06 are obtained by rescaling the LRT-LDA calculated λ and the average frequencies following ref. [14]. LRT-LDA and HSE06 are denoted as LDA and HSE, respectively. Except for the pressure, other quantities are shown for CsTlF$_3$ only considering that the A elements has little effects on the electron-phonon interaction related properties. The lattice constants are about 4.74, 4.69, and 4.66 Å at ambient pressure for A=Cs, Rb, and K, respectively, according to HSE06 calculations.

a (Å)	Pressure (GPa)	REPME (eV/Å)		x	ω_{log} (K)	λ			T_c (K)	
	HSE (Cs/Rb/K)	GGA	HSE			LDA opt	LDA tot	HSE	LDA	HSE
4.60	5.4/3.3/2.3	5.0	8.8							
4.50	12/9.2/7.7	5.5	9.6	0.35	293	0.47	0.55	1.51	5.2	**30**
4.40	19/16/14	6.1	10.3	0.35	377	0.26	0.32	0.81	0.3	**16**

Table 2: The same quantities as in table 1 but for the simple cubic ATlCl$_3$ compound (A=Cs, Rb, and K). Except for the pressure, other quantities are shown for CsTlCl$_3$ only. The corresponding lattice constants at ambient pressure are about 5.53, 5.50, 5.48 Å for A=Cs, Rb, and K, respectively.

a (Å)	Pressure (GPa)	REPME (eV/Å)		x	ω_{log} (K)	λ			T_c (K)	
	HSE (Cs/Rb/K)	GGA	HSE			LDA opt	LDA tot	HSE	LDA	HSE
5.40	2.2/1.6/1.3	4.9	8.1	0.35	142	0.80	0.91	2.32	9.0	**21**
5.30	4.5/3.8/3.5	5.2	8.4	0.35	191	0.47	0.53	1.30	3.1	**17**
5.20	7.4/6.4/5.8	5.5	8.8	0.35	213	0.35	0.40	0.94	0.9	**12**
5.10	11/9.9/9.3	5.8	9.3	0.35	222	0.26	0.33	0.73	0.3	**7.8**

all q points have positive phonon frequencies therefore the 0.35/f.u. hole-doped CsTlF$_3$ and CsTlCl$_3$ compounds in the cubic perovskite structure at the studied volumes are dynamically stable at the LRT-LDA level. A common feature of the phonon spectra is that the phonon frequency of the F-breathing mode strongly softens from the zone center Γ point to the zone boundary M and R points. For example, the phonon frequency of the F-breathing mode strongly softens from about 60 meV at Γ point to only $\sim$23 meV at M and R points in 0.35/f.u. holed doped CsTlF$_3$ as shown in fig. 3(a). Accompanying the softening of the phonon frequency, the F-breathing phonon modes acquire large electron-phonon coupling when approaching the M and R points. This suggests that the F-breathing mode makes a major contribution to the total electron-phonon coupling strength λ, which is further supported from the Eliashberg function $\alpha^2F(\omega)$ shown in fig.3(a). The same feature discussed above is found in CsTlCl$_3$ as well, as shown in fig. 3(b), whereas the phonon frequencies in CsTlCl$_3$ are much smaller than CsTlF$_3$, due to the heavier atomic mass and bigger radius of Cl atom (thus larger equilibrium lattice constant).

In table 1 and 2, we present, respectively, the calculated results of some important quantities for CsTlF$_3$ and CsTlCl$_3$ at various lattice constants and doping levels. For each lattice constant, the corresponding pressure is calculated by DFT-HSE06 with undistorted perovskite structure of the undoped compound. The other quantities included are the REPMEs of the F/Cl breathing mode using DFT-GGA and DFT-HSE06, the average phonon frequency ω_{log}, the electron-phonon coupling $\lambda_{L,o}$ (contributed by optical phonons only) and λ_L (contributed by all phonons) from the LRT-LDA calculations, the estimated total λ within DFT-HSE06, and the superconducting temperature T_c. Since the electron-phonon coupling can be very strong ($\lambda > 1$), we adopt the revised Allen-Dynes formula [33] with μ^*=0.1 to estimate T_c.

We find in the LRT-LDA calculations, that at a fixed volume, the total electron-phonon coupling λ (average frequencies) generally increases (decrease) with decreasing doping level, in accordance with the trend shown in the insert of fig. 1 and consistent with the expectation that the simple cubic perovskite structure become unstable towards smaller doping levels. At a fixed doping level, the total electron-phonon coupling λ generally decreases with decreasing volume (increasing pressure) in both CsTlF$_3$ and CsTlCl$_3$ whereas the average phonon frequencies show the opposite trend, namely, they increase with decreasing volume (increasing pressure) as expected. Therefore, the maximum T_c with varying volume (pressure) relies on the competition between λ and ω_{log}. For the volumes we studied, the LRT-LDA theoretical electron-phonon coupling is

as high as 1 and the maximum T_c reaches about 10 K for $CsTlF_3$ and $CsTlCl_3$, which already suggest that these compounds are good phonon-mediated superconductors. By taking into account non-local correlation effects, the maximum theoretical T_cs estimated by HSE06 are 30 K and 21 K for optimal doped $CsTlF_3$ and $CsTlCl_3$ compounds under about 12 and 2 GPa pressure, respectively. (See table. 1 and 2)

Discussion and Conclusion. – Our results support the validity of the qualitative phase diagram shown in fig.1, and provide quantitative estimates, which should motivate the experimental synthesis of the materials described in this letter. In this class of materials it is important to optimize the volume/pressure to achieve maximum T_c. At large volumes/low pressures, the CDW phase is so stable that it cannot be suppressed by reasonable doping. On the other hand, at very small volumes/high pressures, the electron-phonon coupling become weak and the T_c is vanishingly small. The critical superconducting temperature T_c as high as 30 K and 20 K are expected in optimally doped and compressed $CsTlF_3$ and $CsTlCl_3$, respectively, within the uncertainty of the calculations, which are meant to provide guidance to the experimental search for new superconductors and can be refined by performing larger supercell calculations.

In addition to applying pressure, the volume of the $CsTlF_3$ and $CsTlCl_3$ compounds can be tuned by replacing the Cs atoms with other alkaline atoms such as Rb and K. The HSE06 optimized lattice constants at zero pressure for $RbTlF_3$, $KTlF_3$, $RbTlCl_3$, and $KTlCl_3$ are about 4.69, 4.66, 5.50, 5.48 $\AA$, respectively. On the other hand, replacing F and Cl with Br and I is detrimental for superconductivity due to their heavier masses.

To reach a doping of 0.3-0.4 hole/f.u., it is best to substitute alkaline atoms with vacancies and/or charge neutral units. Doping on the active sites by replacing F/Cl atoms with O/S and/or N/P atoms or substituting Tl by Hg, introduces disorder and removes the active pairing sites. Other avenues for doping should also be explored such as electrostatic gating which was shown recently in ref. [34] to be able to induce superconductivity in $KTaO_3$ at 50 mK.

Our approach for designing novel high-temperature superconductors is quite general and can be used to search for other "other high temperature superconductors".

* * *

Z.P.Y and G.K. were supported by the AFOSR-MURI program towards better and higher temperature superconductors. We are grateful to Mac Beasley and Martha Greenblatt for discussions and a critical reading of the manuscript.

REFERENCES

[1] Ceder G., Aydinol, M. K., and Kohan A. F., *Computational Materials Science*, **8** (1997) 161.
[2] Menga Y. S. and Elena Arroyo-de Dompablo M., *Energy Environ. Sci.*, **2** (2009) 589.
[3] Sato K. and Katayama-Yoshida H., *Semicond. Sci. Technol.*, **17** (2002) 367.
[4] Greeley J. and Mavrikakis M., *Nat. Mater.*, **3** (2004) 810.
[5] Stengel M., Fennie C. J., and Ghosez P., *Phys. Rev. B*, **86** (2012) 094112.
[6] Birol T. *et al.*, *arXiv:1207.5026*, () .
[7] Hasan M. Z., and Kane C. L., *Rev. Mod. Phys.*, **82** (2010) 3045.
[8] Qi X.-L. and Zhang S.-C., *Rev. Mod. Phys.*, **83** (2011) 1057.
[9] Wan X., Turner A. M., Vishwanath A., and Savrasov S. Y., *Phys. Rev. B*, **83** (2011) 205101.
[10] Feng J., Grochala W., Jaroń T., Hoffmann R. , Bergara A., and Ashcroft N. W., *Phys. Rev. Lett.*, **96** (2006) 017006.
[11] Li Y., Gao G., Xie Y., Ma Y., Cui T., and Zou G., *PNAS*, **107** (2010) 15708.
[12] McMahon J. M. and Ceperley D. M., *Phys. Rev. B*, **84** (2011) 144515.
[13] Rosner H., Kitaigorodsky A., and Pickett W. E., *Phys. Rev. Lett.*, **88** (2002) 127001.
[14] Yin Z. P., Kutepov A., and Kotliar G., *arXiv:1110.5751*, () .
[15] Pickett W. E., *Physica B*, **296** (2001) 112-119.
[16] Cava R. J. *et al.*, *Nature*, **332** (1988) 814-816.
[17] Cava R. J. *et al.*, *Phys. Rev. B*, **44** (1991) 9746-9748.
[18] Yamanaka S., *Annu. Rev. Mater. Sci.*, **30** (2000) 53-82.
[19] Krukau A. V., Vydrov O. A., Izmaylov A. F., and Scuseria G. E., *J. Chem. Phys.*, **125** (2006) 224106.
[20] Zhang X. W., Yu L. P., Zakutayev A., and Zunger A., *Adv. Funct. Mater.*, **22** (2012) 1425-1435.
[21] Kojima N., *Bull. Chem. Soc. Jpn.*, **73** (2000) 1445-1460.
[22] Wang S. *et al.*, *arXiv:1205.1077*, () .
[23] Kresse G. and Furthmüller J., *Comput. Mater. Sci.*, **6** (1996) 15-50.
[24] Perdew J. P., Burke K., and Ernzerhof M., *Phys. Rev. Lett.*, **77** (1996) 3865-3868.
[25] Franchini C., Kresse G., and Podloucky R., *Phys. Rev. Lett.*, **102** (2009) 256402.
[26] *www.fiz-karlsruhe.de/icsd.html*, ()
[27] Savrasov S. Y., *Phys. Rev. B*, **54** (1996) 16470-16486.
[28] Perdew J. P. and Wang Y., *Phys. Rev. B*, **45** (1992) 13244.
[29] Kasinathan D. *et al.*, *Phys. Rev. Lett.*, **96** (2006) 047004.
[30] Yin Z. P., Savrasov S. Y., and Pickett W. E., *Phys. Rev. B*, **74** (2006) 094519.
[31] Yin Z. P., Gygi F., and Pickett W. E., *Phys. Rev. B*, **80** (2009) 184515.
[32] Kong Y., Dolgov O. V., Jepsen O., and Andersen O. K., *Phys. Rev. B*, **64** (2001) 020501(R).
[33] Allen P. B. and Dynes R. C., *Phys. Rev. B*, **12** (1975) 905.
[34] Ueno K. *et al.*, *Nature Nanotechnology*, **6** (2011) 408.